EUROfusion

EUROFUSION WP14ER–PR(15)65

A.S. Thrysøe et al.

The Influence of Blobs on Neutral Particles in the Scrape–Off Layer

Preprint of Paper to be submitted for publication in
Plasma Physics and Controlled Fusion

This work has been carried out within the framework of the EUROfusion Consortium and has received funding from the Euratom research and training programme 2014-2018 under grant agreement No 633053. The views and opinions expressed herein do not necessarily reflect those of the European Commission.

The Influence of Blobs on Neutral Particles in the Scrape-Off Layer

Alexander S. Thrysøe[1*], Laust E. H. Tophøj[1], Volker Naulin[1], Jens Juul Rasmussen[1], Jens Madsen[1], Anders H. Nielsen[1]

[1]PPFE, Department of Physics, DTU, DK-2800 Kgs. Lyngby, Denmark

Abstract

Interactions between plasma and neutrals are investigated with particular attention to to the influence of large amplitude blob structures that mediate a significant particle and energy transport through the Scrape-Off Layer (SOL). We perform a statistical analysis of the mean-field approximation for plasma parameters in the SOL, and this approximation is shown to be invalid in a SOL with a high level of fluctuations, as those are strongly correlated. A 1D neutral fluid model which account for both cold and hot neutral is formulated and the effects of blobs on the ionization in the SOL and edge are investigated. Simulations suggest that hot neutrals originating from charge exchange reactions are the main player in plasma fueling, and that the dominating result of blobs in the SOL is an alteration of the hot neutral source. These results are recovered in a simplified 2D model.

1 Introduction

Transport from the bulk plasma edge to the wall of a magnetically confined plasmas is found to be highly intermittent [1, 2, 3]. A significant part of heat and particles are carried across the magnetic field lines in field-aligned filaments of enhanced plasma pressure. Such filaments are usually denoted blobs. The region outside the plasma edge is characterized by open magnetic field lines and referred to as the Scrape-Off Layer (SOL). The plasma temperatures in the SOL are much lower that those of the bulk plasma [1, 2]. This allows for the existence of neutral atoms, which are otherwise not present due to a high ionization rate at temperatures above the ionization energy.

Neutrals can originate from plasma-wall interactions or be puffed into the vessel for fueling or imaging purposes. Another technique for fueling, which is not studied in this paper, is supersonic molecular beam injection which have a directed flow and the neutral molecules are not at room temperature.

*alec@fysik.dtu.dk

The neutrals from gas-puffing are at room temperature and thus the mean-free path for ionization is short compared to the width of the SOL and similar to the perpendicular length scale of blobs [4]. This indicates that the influence of the intermittent structures on the neutrals differs significantly from what one would find from approximating the blobs by mean density and temperature. This is due to the strong dependencies on plasma particle density and temperature of the reaction rates. In a quiet SOL the ionization will be weak due to the low temperature, but the blobs come with a significantly enhanced temperature and density, and thus lead to a significant increase in ionization. Due to the strong dependence of the ionization rate on temperature and density we cannot treat the contribution from the blobs just by a mean-field theory, i.e., average over the the blob density and reaction rate or temperature.

In this paper the feasibility of computing quantities from knowledge of mean fields in the plasma is discussed on the background of results obtained from a numerical edge/SOL turbulence code. We show that the mean-field approximation for the electron impact ionization rate is invalid in the SOL region, due to the strong correlation between plasma density and temperatures in blobs, and the strong temperature dependence of the electron impact ionization rate coefficient.

The blob-neutral interactions are further investigated in a simpler 1D model, that takes into account the most dominant reactions between the plasma and neutral particles. The model includes the hot neutral particles produced in charge exchange collisions between cold neutrals and hot plasma. The results suggest that hot neutrals play an important role in the ionization balance between the edge and SOL regions, since they are not lost at a significant rate in the SOL due to their long ionization mean-free path. Thus, hot neutrals are responsible for the majority of the neutral density flux across the last closed flux surface (LCFS), and are therefore important for plasma fueling. We also find that the fraction of ionization occurring in the SOL increases with the increasing blob frequency.

The structure of the paper is as follows. In Section 2 the interactions between plasma and neutrals are described, and mean-free paths for ionization and charge-exchange interactions at different neutral temperatures are discussed. Section 3 contains critical analysis of the mean-field approach in the SOL. In Section 4 the 1D model is used to analyze the interactions between blobs and neutrals, and we compare the ionization in the SOL and edge regions and the neutral density flux across the Last Closed Flux Surface (LCFS). In this section we also present results from a simplified 2D model and compare those to the 1D results. The conclusions are summarized in Section 5.

2 Plasma-Neutral Interactions

For a given collision reaction between two species of number density n_1 and n_2, the reaction rate is given by

$$\nu_R = n_1 n_2 \langle \sigma_R v_r \rangle, \tag{1}$$

where $\sigma_R = \sigma_R(v_r)$ is the cross-section of reaction R, and v_r is the relative velocity of species 1 and 2. The brackets $\langle \cdot \rangle$ indicate the average over the velocity distributions of the species. The velocity averaged quantity is known as the rate coefficient

$$k_R \equiv \langle \sigma_R v_r \rangle. \tag{2}$$

The rate coefficient thus determines the rate of a given reaction, say electron impact ionization. As long as many-body interactions can be neglected, it is independent of the densities of the species. In the following, we shall discuss the behavior of the reaction rate, and how temporally averaging its factors affect this.

In this paper we assume that the neutrals consist of atomar hydrogen. In actual fueling scenarios molecular gas is injected, and we assume the dissociation of those molecules to occur so far out in the SOL, that it is reasonable to only include the neutral atoms in the model. It should also be mentioned that a proper inclusion of molecular interactions should also account for the energy required to dissociate hydrogen molecules (which is roughly 4.5 eV, see e.g. [5]).

The hydrogen molecule dissociation would also introduce another warm neutral source, since the atoms resulting from the dissociation will carry the molecular binding energy of a few eV. Those neutrals are referred to as Franck-Condon neutrals [6] and they are also not accounted for in this paper.

Simple estimates (see, e.g., [6]) allow for expressing the rate coefficient for electron impact ionization, radiative recombination and charge-exchange for ground-state hydrogen as

$$k_{\mathrm{iz}} = 2 \cdot 10^{-13} \frac{\sqrt{T_\mathrm{e}/T_*}}{6 + T_\mathrm{e}/T_*} \exp\left(-\frac{T_*}{T_\mathrm{e}}\right), \tag{3}$$

$$k_{\mathrm{rc}} = 7 \cdot 10^{-20} \sqrt{\frac{T_*}{T_\mathrm{e}}}, \tag{4}$$

$$k_{\mathrm{cx}} = 8 \cdot 10^{-19} \left(\frac{3}{2} \cdot T_\mathrm{i}\right)^{-0.2} \sqrt{\frac{3T_\mathrm{i}}{m_\mathrm{i}}}, \tag{5}$$

where T_* is the ionization potential (13.6eV for hydrogen). Temperatures are inserted in eV, and the reaction rates have units $\mathrm{m^3 s^{-1}}$. Here, (3-4) are taken from [7], and (5) is taken by assuming the charge-exchange cross section $\sigma = 8 \cdot 10^{-19} (\frac{3}{2} T_\mathrm{i}/\mathrm{eV})^{-0.2}\,\mathrm{m}^2$ estimated from Fig. 10.8 of [7] and using the ion

sound speed. The reaction rates are plotted in Fig. 1. Note that we do not consider the recombination reaction in this paper, as it is several orders of magnitudes smaller than ionization and charge exchange in the domain of interest.

The mean-free path of species 1 for some reaction R with species 2 is given by [7]

$$\lambda^1_{\mathrm{mfp}} = \frac{v_{\mathrm{th}}}{n_2 \langle \sigma_{\mathrm{R}} v_r \rangle}\,, \tag{6}$$

where v_{th} is the thermal velocity of species 1. If the mean free path is larger than the domain, the reaction occurring at an equal rate throughout the system. If on the other hand the mean-free path of neutrals for, e.g., ionization is much smaller than the system, there will be a localized plasma source. In Figure 2a the mean-free path for neutral atoms is shown as a function of plasma temperature and density. It is seen that the cold neutral mean-free path in the SOL is roughly 10 cm for ionization and 5 cm for charge exchange collisions, for typical SOL conditions of medium sized tokamaks. This is smaller than or comparable to the typical SOL width, and this suggests that the flux of cold neutrals across the LCFS is small compared to that of the neutrals puffed into the system. The charge exchange collisions does, however, change a hot ion and a cold neutral to a cold ion and a hot neutral and thus source a warmer species of neutrals, that has a larger mean-free path.

In Figure 2b the ionization mean-free path of neutrals of temperature $T = 50$ eV is depicted. The mean-free path for hot neutrals is much larger than the SOL width, and these are expected to mainly be ionized within the first 10 cm of the edge region.

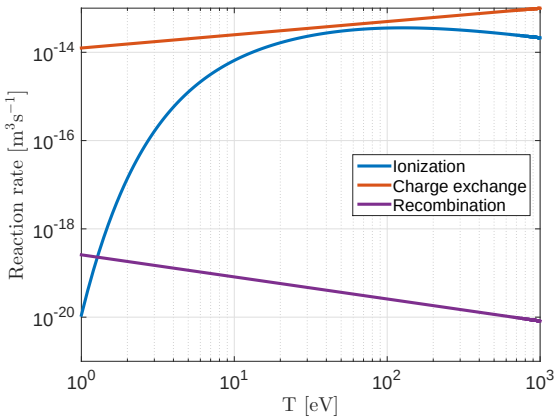

Figure 1: Reaction rates given by (3,4,5). Compare to Stangeby [6], p.35.

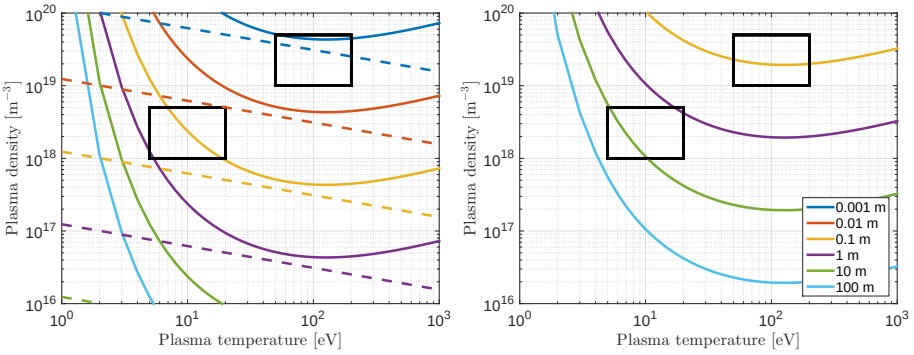

(a) (b)

Figure 2: Mean free paths for cold neutral atoms at $T_\mathrm{n} = 300\,\mathrm{K}$ (a) and hot neutral atoms at $T_\mathrm{n} = 50\,\mathrm{eV}$ (b) for ionization (solid) and charge exchange (dashed) reactions. Note that there are no dashed line in (b), since charge exchange collisions does not affect the hot neutral density. The lower left rectangle indicates the typical SOL parameter domain and the upper right rectangle the typical edge parameter domain.

3 Averaging Correlated Signals

We begin with a generic discussion on averaging of fluctuating signals. Without loss of generality an intermittent field $x(t)$ can be written as the sum of a temporally averaged part $\bar{x} \equiv \langle x \rangle$ and a fluctuation part $\tilde{x}(t)$, as $x(t) = \bar{x} + \tilde{x}(t)$. Note that the average here is different from that defined in the previous section. The average of a product of two signals $x(t)$ and $y(t)$ is

$$\langle x(t)y(t) \rangle = \bar{x}\bar{y} + \langle \tilde{x}\tilde{y} \rangle \,. \tag{7}$$

Expressing the average of the product as the product of the averages, i.e., by ignoring the second term on the right hand side of (7), ignores the *cross-correlation* $\langle \tilde{x}\tilde{y} \rangle$ of the signals. In the case of edge/SOL turbulence, this cross-correlation may be very significant, if the signal relates to, e.g., the density and temperature. Another statistical treatment of blobs is presented in [8], where a stochastic model for the plasma density fluctuations in a single point is presented. A critical assessment of the mean-field approach is also covered in [9]. The conclusions from our analysis of the mean-field approximation are consistent with those presented there.

This feature can be illustrated by a simple example. Consider a signal x having two levels. At a fraction δ of time, $x = X$, and a fraction $1-\delta$ of time, $x = RX$ with $R<1$. We consider the averaging procedure for the square of this signal, as a proxy for two perfectly correlated signals. Now, $\langle x \rangle = [\delta + (1-\delta)R]X$, and $\langle x^2 \rangle = [\delta + (1-\delta)R^2]X^2$, so the difference between including both terms

in (7) and only the first is

$$\frac{\langle x^2\rangle}{\langle x\rangle^2} = 1 + \frac{\delta(1-\delta)}{(\delta+R)^2}\,. \tag{8}$$

Now, for typical SOL conditions found in simulations (cf. Figure 3), $R \sim 5\%$ and $\delta \sim 15\%$, leading to

$$\frac{\langle x\rangle^2}{\langle x^2\rangle} \approx 0.24\,. \tag{9}$$

On the other hand, the average of a single function, say f, of a signal $x(t)$, can be expressed by Taylor-expanding f around $\bar{x}$,

$$\begin{aligned}\langle f(x)\rangle &= \left\langle f(\bar{x}) + f'(\bar{x})\tilde{x} + \frac{1}{2}f''(\bar{x})\tilde{x}^2 + \frac{1}{6}f'''(\bar{x})\tilde{x}^3 + \dots \right\rangle \\ &= f(\bar{x}) + \frac{1}{2}f''(\bar{x})\langle\tilde{x}^2\rangle + \frac{1}{6}f'''(\bar{x})\langle\tilde{x}^3\rangle + \dots\,. \end{aligned} \tag{10}$$

Thus, a simple estimate of $\langle f\rangle$ by $f(\bar{x})$ misses contributions from each moment of $\tilde{x}$. Note that the term linear in $\tilde{x}$ vanishes on average by definition.

Applying this observation to the ionization density at different radial positions in a slab geometry with radial coordinate x, poloidal coordinate y and of poloidal width L_y, one takes the average

$$\langle S(x)\rangle \equiv \frac{1}{L_y T}\int_0^T \mathrm{d}t \int_0^{L_y} \mathrm{d}y \;\; S(x,y,t)\,. \tag{11}$$

Taking S as the plasma density source from ionization of neutrals, we have $\langle S\rangle = -\langle n_\mathrm{n}\, n_\mathrm{e}\, k_\mathrm{iz}(T_\mathrm{e})\rangle$. We expand each physical quantity in a mean and a fluctuation term, i.e. $f \equiv \langle f\rangle + \tilde{f}$, as in (7). Numerical simulations (see Section 4.3) suggest, that the neutral density fluctuations are rather small (of order 10% of the mean) for typical plasma conditions. For now, we therefore neglect these fluctuations, and

$$\begin{aligned}\langle S\rangle &= -\langle n_\mathrm{n}\rangle\langle n_\mathrm{e} k_\mathrm{iz}\rangle \\ &= -\langle n_\mathrm{n}\rangle\left(\langle n_\mathrm{e}\rangle\langle k_\mathrm{iz}\rangle + \langle\tilde{n}_\mathrm{e}\tilde{k}_\mathrm{iz}\rangle\right)\end{aligned} \tag{12}$$

Consider the terms in (12). In a blob-turbulence dominated scenario, the fluctuations of density and temperature are strongly correlated, so we expect the term $\langle\tilde{n}_\mathrm{e}\tilde{k}_\mathrm{iz}\rangle$ to play a major role.

On the contrary, a mean field approach would use only the term $\langle n_\mathrm{e}\rangle\langle k_\mathrm{iz}\rangle$ or $\langle n_\mathrm{e}\rangle k_\mathrm{iz}(\langle T_\mathrm{e}\rangle)$, which might be even worse, due to the strong temperature dependence of k_iz, cf. equation (3).

The strong correlation between the density and the ionization rate coefficient in edge/SOL simulations is shown in the upper frame of Fig. 3. In the bottom frame of Fig. 3 the effect of applying the mean-field approach is demonstrated by comparing the ionization rate to that where the full reaction rate is averaged (solid lines). This result shows that by applying a mean-field approach the average ionization rate is about a factor of 4 too low in the SOL region, consistent with what was estimated in (9).

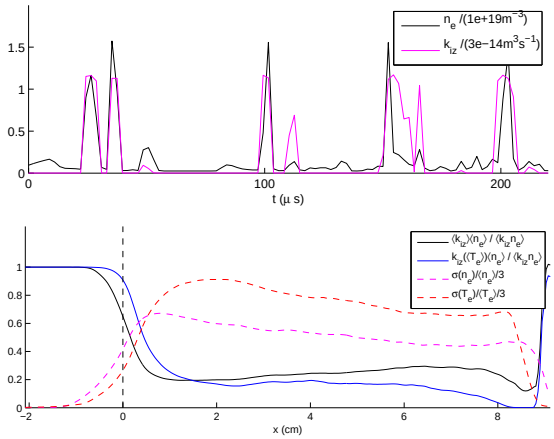

Figure 3: The effect of fluctuations on the ionization rates. **Top:** Time signals of plasma density and ionization rate coefficient $k_{\mathrm{iz}} = \langle \sigma v_{rel} \rangle$ at a fixed position $x = 2\,\mathrm{cm}$, $y = 2\,\mathrm{cm}$. The fluctuations in density and rate coefficient are clearly highly correlated. **Bottom:** Radial (y-averaged) profile of the approximations $\langle n_{\mathrm{e}} \rangle \langle k_{\mathrm{iz}} \rangle$ (black curve) and $\langle n_{\mathrm{e}} \rangle \, k_{\mathrm{iz}}(\langle T_{\mathrm{e}} \rangle)$ (blue curve) normalized by the actual ionization rate per neutral atom $\langle n_{\mathrm{e}} k_{\mathrm{iz}}(T_{\mathrm{e}}) \rangle$, cf. (12). Both approximations underestimate the ionization rate by a factor of about 4 over most of the SOL, where the fluctuations (dashed lines) dominate the mean fields. The plasma conditions are taken from HESEL simulations, cf. section 4.3.

4 1D model

In order to illustrate the influence of blobs on the ionization we start from a simplified 1D model. The radial evolution is modeled in a domain extending from 10 cm inside the plasma edge and out to the wall. This allows for modeling the SOL dynamics as well as comparing ionization profiles for the SOL and edge regions. The model represent the plasma as a static profile with a fixed density and temperature in the SOL and in the edge regions. To model the blob, we consider a Gaussian perturbation of density and temperature in the SOL propagating radially outwards.

The neutrals are assumed to evolve according to diffusion with an effective diffusion coefficient, and are modeled as a 3-species fluid with a different temperature for each species. This assumption gives a simplified description of neutrals compared to that of a kinetic model, but we trust that it bears out the key issues and conclusions in a qualitative way. A diffusion driven transport of neutrals is also investigated in [10], and another model for multi-species neutrals is applied in [11]. The cold neutrals are at room temperature and enter the system at the outer wall. Through charge exchange collisions with the plasma the cold neutrals are either converted into warm neutrals at SOL temperature or hot neutrals at edge temperature. The warm neutrals are created in charge exchange collisions with the SOL background plasma and the hot neutrals from collisions with the edge plasma and the blobs. The diffusion equation for the neutrals can be written

$$\partial_t n_\sigma - \partial_x \left(D_\sigma \partial_x n_\sigma \right) = S_\sigma \,, \tag{13}$$

where $\sigma = \mathrm{n_{cold}}, \mathrm{n_{warm}}, \mathrm{n_{hot}}$. The diffusion coefficient is given by

$$D_\sigma = \frac{T_\sigma}{k_{\mathrm{eff}} m_\sigma n} \,, \tag{14}$$

where k_{eff} is some effective reaction rate coefficient driving the effective diffusion, m_σ is the mass of the neutrals and n is the sum of all densities. The sources and sinks on the RHS of (13) are characterized by the ionization and charge exchange collisions and is given by

$$S_{\mathrm{n_{cold}}} = -\left(k_{\mathrm{cx}} + k_{\mathrm{iz}}\right) n_{\mathrm{n_{cold}}} n_{\mathrm{p}} \,, \tag{15}$$

$$S_{\mathrm{n_{warm}}} = k_{\mathrm{cx}} \left[\left(n_{\mathrm{n_{cold}}} + n_{\mathrm{n_{hot}}} \right) n_{\mathrm{p_{bkgd}}} - n_{\mathrm{n_{warm}}} n_{\mathrm{p_{blob}}} \right] - k_{\mathrm{iz}} n_{\mathrm{n_{warm}}} n_{\mathrm{p}} \,, \tag{16}$$

$$S_{\mathrm{n_{hot}}} = k_{\mathrm{cx}} \left[\left(n_{\mathrm{n_{cold}}} + n_{\mathrm{n_{warm}}} \right) n_{\mathrm{p_{blob}}} - n_{\mathrm{n_{hot}}} n_{\mathrm{p_{bkgd}}} \right] - k_{\mathrm{iz}} n_{\mathrm{n_{hot}}} n_{\mathrm{p}} \,, \tag{17}$$

where $n_{\mathrm{p_{blob}}}$ is the density of the perturbation, $n_{\mathrm{p_{bkgd}}}$ is the plasma background density and $n_{\mathrm{p}} = n_{\mathrm{p_{bkgd}}} + n_{\mathrm{p_{blob}}}$ is the total plasma density. The rate coefficients are calculated from the proper temperatures, i.e., $k_{\mathrm{iz}} n_{\mathrm{p_{bkgd}}}$ is calculated using the background temperature, whereas $k_{\mathrm{iz}} n_{\mathrm{p_{blob}}}$ is calculated from the blob temperature. An example of the profiles during a blob event is given in Fig. 4. It should be noted that the profiles are naturally dependent on the temperatures and plasma density chosen - in this paper we use $n_{\mathrm{p_{bkgd}}} = 2 \cdot 10^{19}\,\mathrm{m}^{-3}$ for the plasma edge background density, $n_{\mathrm{p_{bkgd}}} = 1 \cdot 10^{18}\,\mathrm{m}^{-3}$ for the density in the SOL, and $T_{\mathrm{n_{hot}}} = 40\,\mathrm{eV}$, $T_{\mathrm{n_{warm}}} = 10\,\mathrm{eV}$ and $T_{\mathrm{n_{cold}}} = 25\,\mathrm{meV}$ for the neutral temperatures. We are using an effective reaction rate coefficient for the neutrals of $k_{\mathrm{eff}} = 5 \cdot 10^{-14}\,\mathrm{m^3 s^{-1}}$.

The neutral density boundary conditions on the inner boundary are

$$\partial_x n_\sigma = \sqrt{\frac{k_{\mathrm{iz}} n_{\mathrm{p}}}{D_\sigma}} n_\sigma \,, \tag{18}$$

for $\sigma = \mathrm{n_{warm}}, \mathrm{n_{hot}}$, which is found by assuming that the neutral density is going to zero far in the edge due to ionization and

$$n_{\mathrm{n_{cold}}} = 0\,. \tag{19}$$

On the wall we assume partial absorption of neutrals and thus

$$-\partial_x n_\sigma = -\frac{\gamma}{D_\sigma}\sqrt{\frac{T_\sigma}{2\pi m_\mathrm{n}}} \tag{20}$$

for $\sigma = \mathrm{n_{warm}}, \mathrm{n_{hot}}$ and with $\gamma = 0.5$, and

$$-\partial_x D_{\mathrm{n_{cold}}} n_{\mathrm{n_{cold}}} = 10^{22}\,\mathrm{m^{-3}s^{-1}}\,, \tag{21}$$

to represent a cold neutral influx from, e.g., gas puffing.

4.1 Ionization in SOL and edge

It is important to provide an estimate of the radial distribution of the plasma source from ionization of neutrals in a tokamak device. This can for example be used for the purpose of estimating fueling rate if using gas puffing in future machines such as ITER and beyond.

Using the model described in Section 4 we simulate the neutral response to a series of blob events appearing with a given frequency. This allows for computing the ionization source profiles. The inclusion of hot neutrals in the model also allows for insight into the fueling mechanism. It is expected from Fig. 2 that hot neutrals will penetrate far deeper into the edge region and thus contribute with a larger fraction of ionization in the edge than cold neutrals.

In Figure 4 we show profiles of the densities in the SOL and edge regions. The left column depicts profiles for when the blob is near the edge of the plasma, and the right column when the blob is near the chamber wall. In the top frames of Fig. 4 the plasma density profiles are displayed, and the position of the blob can easily be seen.

In the middle frames the neutral densities are shown. It is observed that the cold neutral density falls off exponentially in the SOL, whereas the warm and hot neutral density is roughly constant in this region. The density of warm and hot neutrals then falls off exponentially in the edge region. The observed results reflect the despondencies of the mean-free paths shown in Fig. 2. It is also noted that while the blob only weakly perturbs the cold neutral density profile, the level of warm and hot species rises globally in the SOL region when the blob reaches the area of high cold neutral density. The increase is caused by an increment of the charge exchange reaction rate, and thus the warm and hot neutral density source, in the presence of a blob.

The bottom frames of Fig. 4 depict the ionization rate during the blob event. As one may expect the ionization in the SOL rises significantly when the blob

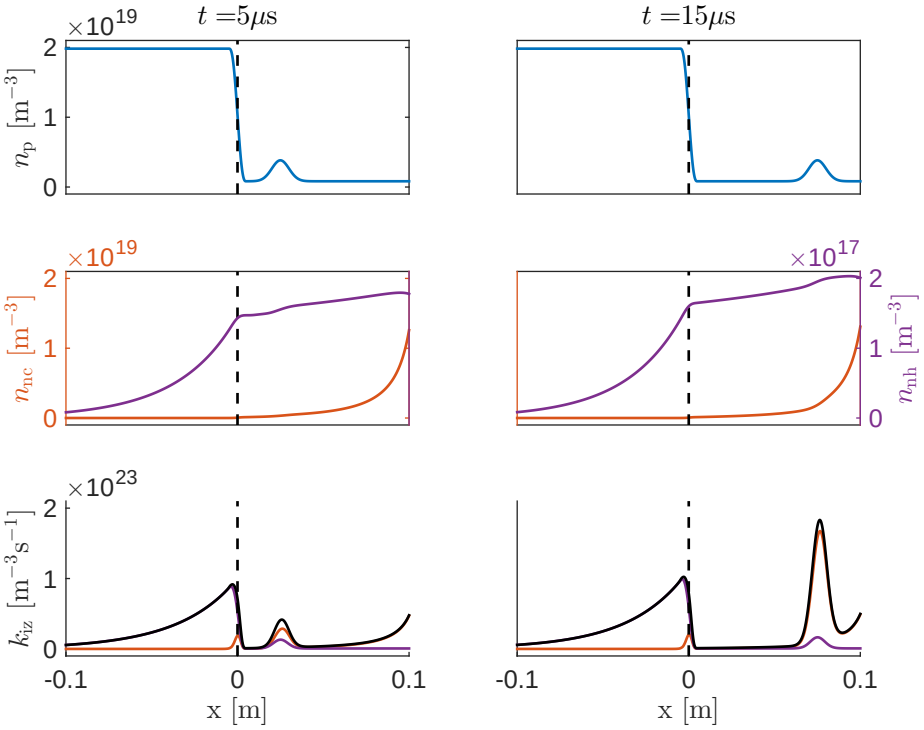

Figure 4: Plasma (top), and cold and sum of warm and hot neutrals (middle) density profiles during a blob event. The bottom frames depict ionization rates for the cold and the sum of warm and hot neutrals for the two blob positions. In the middle and bottom frames the red curves refer to cold neutrals, the purple curves to warm and hot neutrals and the black curves to the sum of all neutrals. Notice that the axis for hot neutral density is two orders of magnitudes smaller than that for cold neutral density.

reaches the regions of high neutral density. However, since more warm and hot neutrals are produced, the flux of neutrals across the LCFS rises, leading to a larger neutral density, and thus ionization rate, in the edge region as well. Thus blobs do not only increase the ionization in the SOL but also that in the edge.

Note that the fluctuation level of the 1D model is much lower than that produced by the HESEL code, which were used to construct Fig. 3.

Figure 5a depicts the same type of profiles as in the bottom frames of Fig. 4, except that the profiles have been averaged over a full blob period. The frequency of the blob events applied in this case is 10 kHz. Is is observed that the the ionization of cold neutrals dominate in the SOL region, whereas the ioniza-

tion of hot neutrals dominate the edge region. This along with the conclusions drawn from Fig. 4 suggest that the location of the cold neutral ionization source only influences the fueling properties weakly. The main role of the cold neutrals in relation to fueling is to act as source for the warm and hot neutrals, and since their mean-free path is much larger than the width of the SOL, the actual location of the source matters very little.

Spatially integrating the profiles reveals that roughly $\frac{1}{3}$ of the ionization occurs in the SOL, and $\frac{2}{3}$ in the edge region. The same procedure have been carried out for various blob frequencies and Fig. 5b reveals a tendency that the higher frequency, the larger a fraction of neutrals are ionized in the SOL. The reason for this is that the cold neutral density do not have time to recover from a blob event when the frequency is higher, and thus the warm and hot neutral source is lower, leading to less neutrals across the LCFS and thus a lower fueling efficiency in the edge region.

Thus in a SOL with more frequent blob events, the ionization rises compared to that in the edge and is in general higher than that of a SOL where the plasma profiles are temporarily averaged. An equivalent conclusion has been made in e.g. [12, 13], where it is found, that including fluctuations instead of using averaged values moves the ionization source outwards towards the wall.

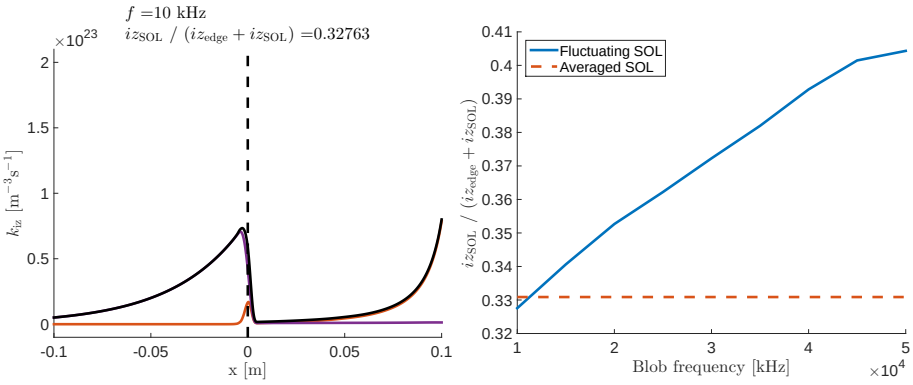

(a) (b)

Figure 5: The ionization rate for the event pictured in Fig. 4 averaged over a blob period (a), where the colors have the same meaning as in Fig. 4, and the fraction of averaged ionization in the SOL as a function of blob frequencies (b).

4.2 Neutral Flux across LCFS

As a continuation of Section 4.1 it is of interest to monitor the neutral flux across LCFS as function of time. This quantity can also serve as a proxy for the fueling rate, if it is assumed that all neutral particles crossing LCFS are ionized in inside the bulk plasma.

The inward neutral density flux across LCFS as a function of time is shown in Fig. 6a for a blob frequency of 10 kHz, i.e., every 100 μs a new blob emerges and propagates through the SOL. As explained in Section 4.1 the blob generates an increased amount of hot neutrals when reaching the region of high cold neutral density. This is expressed in the neutral flux plot as a peak approximately 20 μs after the blob is released.

This peak is followed by a period of reduced flux; as the blob propagates through the SOL it ionizes and thus partially empties the SOL for cold neutrals. The lowered cold neutral density result in a lower warm and hot neutral generation and thus a smaller flux across the LCFS. As the cold neutrals are repopulating the SOL after a blob event the flux rises to the non-perturbed value.

As was done for the ionization rates in the previous section, the inward neutral density flux for various blob frequencies are compared. The result is shown in Fig. 6b. It is observed that the neutral flux across LCFS decreases with increasing blob frequency. The reason for this is that for a shorter blob period the cold neutrals will not have time to build up the steady state density and the amount of warm and hot neutrals produced during the next blob is smaller.

The results from this and the previous section suggest that warm and hot neutrals produced in charge exchange collisions are responsible for the majority of the ionization in the edge region. During a blob event, more hot neutrals are produced with the effect that the fueling rate increases. However, after the blob event the SOL has been partially emptied for cold neutrals, leading to a lower fueling rate while the steady state rebuilds.

4.3 Comparison with 2D model

Blobs are localized in time, and spatially in the poloidal plane perpendicular to the magnetic field. By determining the effect of blobs from a 1D model, one undesirably neglect important dynamics that are present in higher dimensions. In particular it is observed, that in the 1D model the blob partially empties the SOL from cold neutrals as it propagates through. Refilling of the void behind the blob with cold neutrals only happens effectively when the blob is in the far SOL, as the cold neutrals do not have a mean-free path long enough to refill through the SOL. However, in a 2D slab model the refilling is assisted by the surrounding cold neutrals and not only those in front of the blob. This allows for maintaining a more constant level of cold neutral density and the decrease in

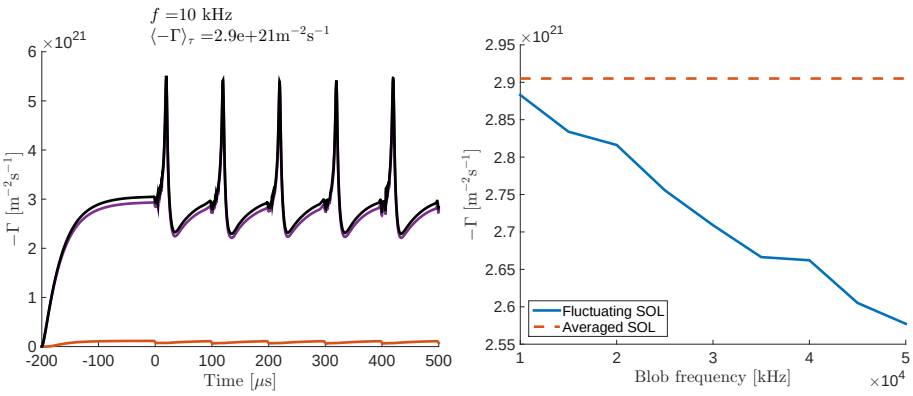

(a) (b)

Figure 6: The inward neutral density flux across LCFS as a function of time (a), where the colors have the same reference as in Fig. 4, and the average flux during a blob period as a function of the blob frequency (b).

neutral flux across the LCFS after a blob event do not occur to the same extent. Note that extending from a 2D model to a full 3D model is not expected to influence the results significantly, since the blob is elongated along the direction parallel to the magnetic field lines, which reduces the cold neutral density by ionization, and thus its ability to refill from this direction.

The simplified 2D model is similar to the 1D model. The plasma density and temperature profiles are fixed and constant in the poloidal direction, and blobs are modeled as 2D Gaussian perturbations that propagate radially outwards. The blobs are born at random poloidal positions at a specified frequency. The neutral transport equations are 2D versions of (13), that also include diffusion in the y-direction (poloidally) with the same diffusion constant, given by (14).

Figure 7 shows the plasma density during a blob event, and the neutral flux across the LCFS. The latter is observed to be significantly different from that of the 1D model. Even though the peak and valley signature of a blob on the neutral flux across LCFS is still visible, this is strongly weakened in a 2D model.

The reason for this is that cold and hot neutrals can flow to and from the regions of increased or decreased density also in the poloidal direction and the domain/blob area ratio is much larger. This allows more neutrals to distribute themselves across the SOL as well as aids to fill up regions of depletion.

Lastly we show in Fig. 8 that the localized ionization is also present in more realistic blob simulations. Here we show results from a HESEL simulation

[14, 15], where neutrals have been added to react to the plasma temperature and density, but without affecting the plasma. The left column of frames shows the plasma density and temperature produced in the HESEL simulation. Note the blob emerging at the edge as well as the one in the SOL at $x = 6\,\mathrm{cm}$ from the LCFS. The upper right frame depicts the total neutral density and the lower right the ionization of the neutrals.

This figure serves as initial results of work in progress, in which we self-consistently couple the neutral model to the HESEL equations, and also include the effects of the plasma produced by impact ionization and the effects of the neutrals on the blobs and the SOL power deposition profile, to obtain a realistic plasma source profile.

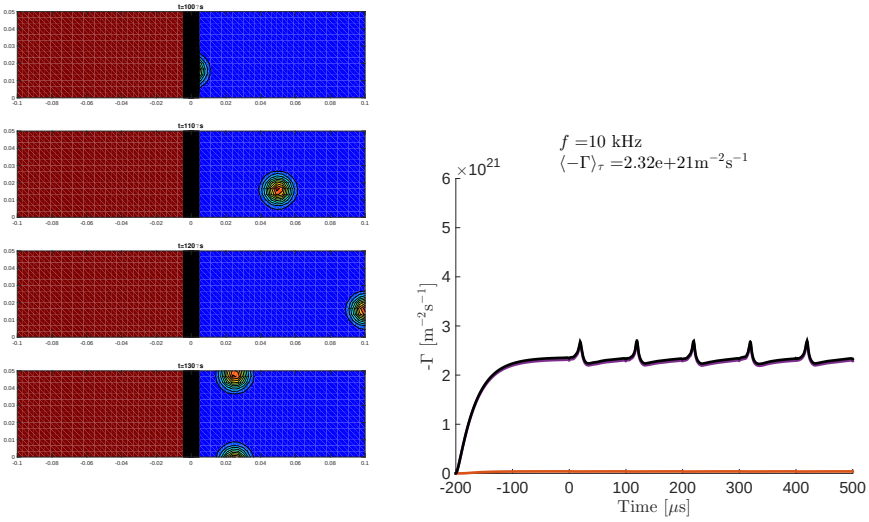

(a) (b)

Figure 7: Plasma density at various times in 2D simulation (a), and the poloidally averaged inward neutral density flux across LCFS as a function of time (b). Compare the latter to Fig. 6a.

5 Conclusions

The mean-field approximation, in which the plasma density and temperature or reaction rate coefficients are approximated separately by their temporal mean values, in the SOL was studied. Based on analytical estimates as well as results from the edge/SOL turbulence code HESEL, it was found that the mean-field approximation is poor in the SOL due to strong correlation between the fluctuating signals. Applying the mean-field approximation for the profiles obtained

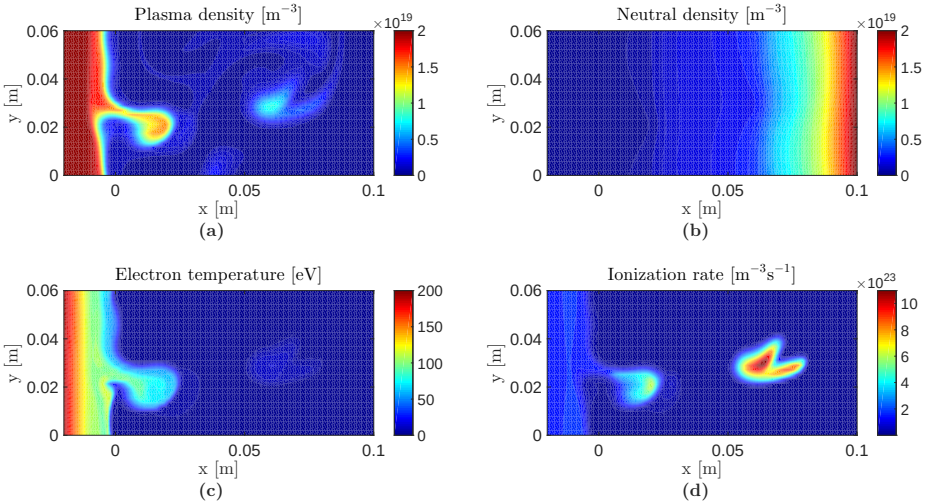

Figure 8: **Left:** Plasma density and temperature plots obtained by solving the HESEL equations numerically. These consist of a self-consistent description of electron density, electron and ion temperature, and vorticity. **Right:** Neutral density (both cold, warm and hot) and ionization rate calculated as response to HESEL output, but without feedback to the plasma. The neutral model is identical to that of used in Fig. 7.

by HESEL simulations led to an electron impact ionization rate that was only about 25 % of the value obtained when taking the proper temporal average throughout the SOL.

We have introduced a radial 1D model for plasma and neutrals in the SOL and edge regions. The model includes three neutral species of room-, SOL- and edge-temperatures. The latter two species originate from charge exchange collisions between plasma and room-temperature cold neutrals. The model was used to study the effect that the frequency of blobs and thereby the fluctuation level in the SOL had on neutral atoms. It is found that more frequent blob events increase the fraction of ionization in the SOL and thus moves the ionization source outwards.

The 1D model also allowed for investigating the neutral density flux across LCFS. This is an interesting measure, as it is closely related to the fueling process of, e.g., gas puffing in tokamaks. It was found that the neutral inward flux at LCFS from hot neutrals is dominating over that of cold neutrals, and hot neutrals are thus vital in the gas puff fueling process. We saw that during a blob event more hot neutrals are produced, which increases the flux across LCFS, but the flux falls to under the steady state level after a blob event. The

latter is because the cold neutral density, which source the hot neutrals, has been depleted by the increased ionization from the blob.

Finally, the results of the 1D model were compared to those of both a similar simplified 2D model and those obtained from HESEL simulations. We see that the above trends also show up in 2D models, but that for example the perturbations to the neutral flux across LCFS are weaker.

Current and future work concerns a self-consistently coupling of the neutral model to the HESEL equations, which will also include the effect of the impact ionization on the plasma and thus the effects of the neutrals on the blobs.

Here we have considered L-mode like plasmas with significant blob activity. One should expect that the ELM events in H-mode plasma may have similar and even stronger effects. The ELM events appear as a bunch of filamentary structures having similar features as blobs. Thus, with their significantly enhanced level of density and temperature - comparable to the parameters on top of the edge pedestal - we expect ELM filaments to locally fully ionize the cold neutrals in the SOL. The charge exchange collisions will additionally produce very hot neutrals, and it is therefore also expected that ELMs will give rise to an increased fueling deep into the edge plasma. This will provide a modulation of the fueling with a frequency determined by the ELM frequency. Thus, the influence of the ELMs may be traced far into the plasma by the modulation of the inward moving plasma density perturbations. Additionally, the enhanced ELM- fueling may add to a faster recovery of the pedestal.

6 Acknowledgments

This work has been carried out within the framework of the EUROfusion Consortium and has received funding from the Euratom research and training programme 2014-2018 under grant agreement No 633053. The views and opinions expressed herein do not necessarily reflect those of the European Commission.

References

[1] Zweben, S.J., et al., Plasma Phys. Control. Fusion, 49 (2007), p. S1

[2] Boedo, J.A., J. Nucl. Mater., 390391 (2009), p. 29

[3] Naulin, V., J. Nucl. Mater., 363365 (2007), p. 24

[4] Boedo, J.A., J. Nucl. Mater., 390391 (2009), p. 29

[5] Darwent, B.deB., Bond Dissociation Energies in Simple Molecules, US Department of Commerce, (1970).

[6] Stangeby, P.C., The Plasma Boundary of Magnetic Fusion Devices, Institute of Physics Publishing, (2000).

[7] Goldston, R.J. and Rutherford, P.H., Introduction to Plasma Physics, IOP Publishing Ltd, (1995).

[8] Garcia, O.E., Physical Review Letters 2012, Volume 108 (26)

[9] Havlíčková, E., et al., Journal of Nuclear Materials, Volume 415, Issue 1, Supplement, 1 August 2011, Pages S471-S474

[10] Vold, E.L., et al., Journal of Nuclear Materials, 176:570-577, December 1990

[11] Tokar, M.Z., Phys. Plasmas 21, 082517 (2014)

[12] Guzmán, F., et al., Journal of Nuclear Materials, Volume 463, August 2015, Pages 659-663

[13] Bernert, M., et al., Plasma Physics and Controlled Fusion, Volume 57, Issue 1, 2015

[14] Garcia, O.E., et al., Phys. Plasmas, 12 (2005), p. 062309

[15] Neilsen, A.H., et al., Conference Paper 40th European Physical Society Conference on Plasma Physics, Espoo, Finland (2013)